





Article

The Mediterranean Coast of Andalusia (Spain): Medium-Term Evolution and Impacts of Coastal Structures

Rosa Molina ¹, Giorgio Anfuso ^{1,*}, Giorgio Manno ² and F. Javier Gracia Prieto ¹

¹ Department of Earth Sciences, Faculty of Marine and Environmental Sciences, University of Cádiz, Polígono del Río San Pedro s/n, 11510 Puerto Real, Spain

² Department of Engineering, University of Palermo, Viale delle Scienze, Bd. 8, 90128 Palermo, Italy

* Correspondence: giorgio.anfuso@uca.es; Tel.: +34-956-016167

Received: 21 May 2019; Accepted: 21 June 2019; Published: 27 June 2019



Abstract: This paper shows coastal evolution along the Andalusia Region (Spain) and the impacts on it of coastal structures. The study area was divided into 47 units to calculate the erosion/accretion/stability (or evolution) rates by using the DSAS extension of ArcGIS software. Evolution rates were divided into different classes from “Very high accretion” to “Very high erosion”. As a result, 9 units recorded accretion, 19 stability and 19 erosion. Further, 17 units presented a positive balance and 28 units a negative one, showing a negative net balance of 29,738.4 m²/year corresponding to the loss of 1784.30 km² of beach surface in the 1956–2016 period. The distribution of evolution areas along the studied coast was carried out by means of the “R” project for statistical computing. The analysis evidenced the impact of rigid structures: accretion was essentially observed up-drift of ports and groins and in correspondence of protection structures, especially of breakwaters. Erosion classes were observed down-drift of ports and groins and in correspondence of revetments/seawalls, and at largest river deltas, and “stability” was observed at pocket beaches and coastal areas locally stabilized by protection structures. Last, results were used to determine the distribution of swash- and drift-aligned coastal sectors and main direction of sedimentary transport.

Keywords: coastal evolution; DSAS; groin; port; pocket beach; river delta

1. Introduction

Over past decades, coastal erosion related impacts on the world shorelines have been significantly growing due to ongoing coastal development and tourist occupation [1–3] as well as to climatic change-related processes [4], such as sea level rise, the increasing height of extreme waves, or changes the frequency of storms and their intensity [5–8]. This has enhanced scientific interest on the effects of coastal erosion processes, which have been investigated over various time-scales using a variety of methods and data sets according to the study time spans [9–13].

Studies on short-term shoreline dynamics are usually carried out at small spatial scales, during a time span of less than 10 years [10], by using beach topographical profiling or 3D surveys, repeated at regular intervals [12,14–16]. Vertical aerial photographs, satellite images, maps and charts are very useful tools for the reconstruction of coastline changes at long (>60 years) and medium (between 60 and 10 years) temporal scales and large spatial scales [10,17–19].

The prediction of the future coastline trend must be based on the study of coastal changes which have occurred in the recent past taking into account a comparable time scale [20]. This is of especial interest in tourist areas because of the potential damage to human structures and related economic activities and the loss of beaches, which are considered as a major player in tourist markets [21] since

they are worth billions of tourist dollars [22]. As an example, in Spain, France, Italy, Greece and Turkey, tourism receipts account for some 5% of the gross domestic product [23], these countries accounting for “the most significant flow of tourists, a sun, sea and sand (3S) market” [24].

Over the last decades, the Andalusia Mediterranean coast (Spain) recorded one of the fastest rates of urban development along the Spanish littoral and even in Europe. In the Costa del Sol (Málaga Province), population reached 1,136,712 [25] and population increase continued at an annual rate of 9.2% between 2006 and 2011—corresponding to 50% of the demographic increase recorded along the Andalusia littoral during the same period [26]. Nowadays, Costa del Sol receives ca. 10,000,000 visitors per annum, i.e., 35% of all Andalusia visitors, making it one of the most important tourist destinations in Europe.

Regional-scale studies on shoreline rates of change are scarce, despite their high relevance. Some attempts have been made in the USA [27] and Europe [28]. However, inter-comparison of data is not easy since aspects such as shoreline definition or dataset formats are very different from diverse studies [29]. Much work is still needed at a regional/national scale to define the best procedure in regional coastal erosion studies and to obtain a broad view of the regional/local factors affecting short- to medium-term coastal evolution. These data would help in the identification of the main causes of coastal erosion in recent decades.

In this paper, aerial orthophotographs integrated into a GIS project, were used to reconstruct shoreline evolution during a 60-year period in the Mediterranean coast of Andalusia, a more than 500 km long sector of the southern Iberian coast. Special attention was devoted to investigate the impacts of ports and rigid protection structures on coastal evolution. In fact, the studied coast experienced significant erosion problems related to the large developments built during recent decades, primarily the construction of ports, harbors, groins and human settlements [30,31]. All those structures, especially ports and groins, have produced a great impact on the littoral drift, as observed in similar Mediterranean areas by the authors of [32–36]. Additionally, quantification of erosion rates in the studied area is very important because shoreline retreat takes place over a human time-scale. Consequently, the recorded data can be used to determine safe construction setbacks, to evaluate the efficiency of coastal protection structures, and to elaborate coastal erosion management and land use plans [22,37,38].

2. Study Area

The littoral of Andalusia extends along the Atlantic Ocean, the Gibraltar Strait and the Mediterranean Sea (Spain, Figure 1). The Mediterranean littoral is 546 km in length and extends from Gibraltar Strait to the Murcia Region, administratively including the provinces of Cádiz, Málaga, Granada and Almería. It has a prevailing rectilinear E-W outline, with two NE-SW easterly facing sectors, one near the Gibraltar Strait and the other in the easternmost sector (Almería coast).

Coastal orography is dominated by the Betic Range, a tectonically active mountain chain that reaches high elevations close to the coast (more than 2200 m a.s.l. at some points). The coast is irregular and shows cliffs, embayments and promontories. Several small coastal plains develop at the foot of these coastal mountains, especially extended at the mouth of short rivers and *ramblas* draining the chain, the most important being Guadiaro, Guadalhorce, Guadalfeo, Adra and Andarax rivers (Figure 1). Some of them develop wave-dominated deltas at their mouths, as a response to the important water erosion affecting their respective catchments, all of them affected by a typical semiarid climate. Especially under episodic heavy rainfalls, reworked fluvial sands and gravels constitute important sediment supplies to the beach system. In the last decades, river basin regulation plans involving water management for tourist and agricultural purposes, has brought to the construction of dams and reservoirs that have systematically limited sediment supplies to the coast and have promoted coastal retreat in most deltas of the region [30,39,40].

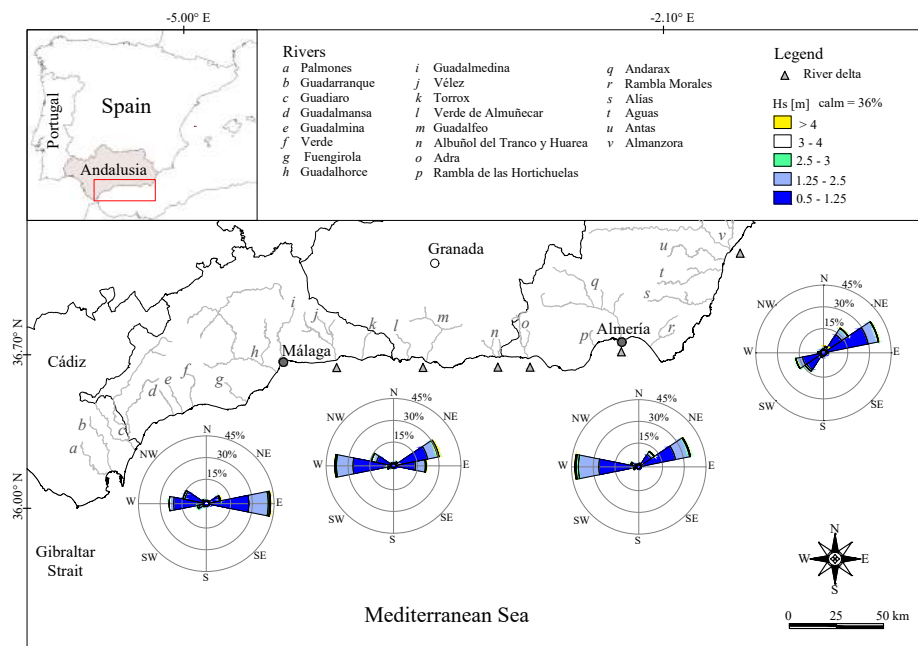


Figure 1. Location map with wave roses for four prediction points.

Beaches are usually composed of medium to coarse dark sands and/or pebbles at *ramblas* mouths. They are often interrupted by rocky sectors and headlands that give rise to pocket beaches (*calas*) of different sizes. Beaches generally show intermediate to reflective morphodynamic states [30].

The coast is a micro-tidal semidiurnal environment (tidal range < 20 cm) [41] exposed to winds blowing from SE to SW with minimum and maximum velocities ranging from 0.4 to 9.0 m/s. The wave climate and storm energy, along the Andalusian coast is very variable [42]. The coasts close to Gibraltar Strait are mainly affected by eastern storms, whereas the central coasts (Málaga and Almería areas) are exposed both to western and eastern storms. Finally, the easternmost portion of the Andalusian coast (Figure 1) is NNE–SSW oriented and primarily exposed to eastern storms [42].

Waves show a clear seasonal behavior with storm conditions being recorded during November–March (i.e., the winter season [30,43]). Due to shoreline orientation, predominant easterly winds and associated storm waves give rise to sea wave conditions generating a prevailing westward littoral drift [43]. Winds from western directions and associated sea waves as well as swell waves that only rarely filter from the Atlantic Ocean, give rise to an opposing drift, which is particularly important in certain coastal sectors and/or periods [30].

3. Methodology

A general evaluation of the erosion/accretion state of the Andalusia coast was previously made by REDIAM Red [44], although only aerial photographs taken in 1977 and 2009 were used; some more detailed analysis at given problematic areas included data from 1956. In this study, aerial orthophotographs from five different years (i.e., 1956, 1977, 2001, 2010 and 2016) and scales (Table 1) were used to reconstruct and quantify shoreline evolution over a medium-term period (60 years, according to criteria proposed by Crowell et al. [10]). Photo interpretation and Geographic Information System (GIS) methods were applied for data processing. The orthophotos were obtained by the Web Map Services (WMS) developed by the Junta de Andalucía (i.e., the Regional Government) following the Open Geospatial Consortium (OGC) interoperability standards. All information was presented in metric Projected Coordinate System WGS84, UTM zones 29 N and 30 N.

Table 1. Characteristics of aerial orthophotographs used. Available online at the website: <http://www.juntadeandalucia.es>.

Year	Flight	Colour Film	Scale	Spatial Resolution (m)
1956	1956–57	Black and white	1:10,000	1.0
1977	Iryda flight 1977–83	Black and white	1:5000	0.5
2001	2001–02	Colour	1:10,000	0.5
2010	PNOA 2010–11	Colour	1:10,000	0.5
2016	PNOA 2016	Colour	1:5000	0.25

The Andalusia shoreline is composed by cliffed (ca. 195 km, marked with a coarser line in Figure 2) and sandy sectors (ca. 350 km). Cliff sectors evolution was not quantified because their changes were within the accuracy of the method used. The temporal and spatial coastal evolution of the rest of the coast was covered by this paper except for a few sectors that were not included due to their small spatial dimension and/or the absence of aerial orthophotographs. The most important beach systems evolution was analyzed by dividing the studied area into 47 units, limited by natural or artificial structures (Table A1). Shore-normal transects were drawn at each unit with a spacing fixed at 25 m, obtaining a total of 11,494 transects along 284.95 km of coastal length (Figure 2).

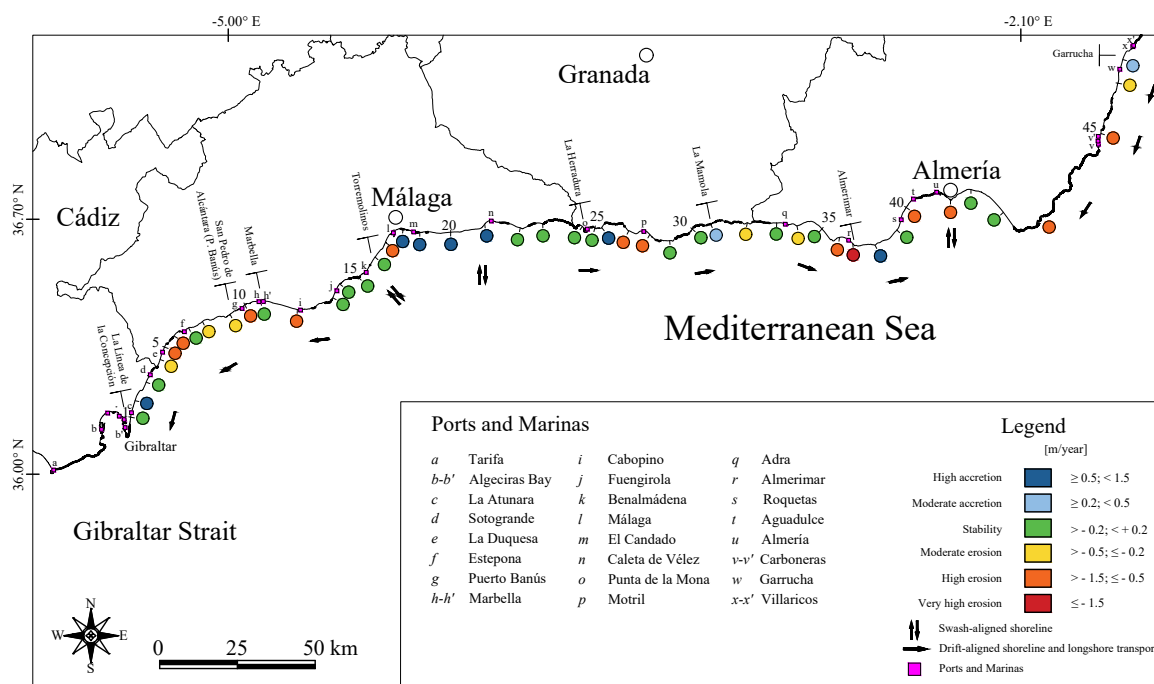


Figure 2. Distribution and characteristics of investigated units, indication of areas with a clear drift-aligned (marked with an arrow showing the prevalent longshore transport direction) or swash-aligned (marked with shore normal double arrows) shoreline trends, location of ports and cliff sectors (marked with a coarser shoreline).

Computation of change rates between shorelines at each transect was made by using the DSAS extension of ArcGIS [45,46] by calculating the Shoreline Change Envelope (SCE) and the Net Shoreline Movement (NSM) [47]. The SCE method deals with variability at each transect taking into account the maximum spatial recorded displacement of shoreline, regardless of the time span along which it was recorded. The NSM is associated with the dates of only two shorelines and it reports the distance between the oldest (1956) and youngest (2016) shorelines for each transect although this movement may be not the maximum shoreline displacement recorded.

Erosion/accretion/stability (or evolution) rates were obtained by using [48]: (i) the “Weighted Linear Regression” (WLR), e.g., more reliable data are given greater emphasis or weight towards determining a best-fit line and considers all used shorelines; (ii) the “Linear Regression Rate” (LRR), which is determined by fitting a least-squares regression line to all shoreline points for a particular transect; and (iii) the “End Point Rate” (EPR), which is calculated by dividing the distance of shoreline movement by the time elapsed between the oldest and the most recent shoreline.

The precision and accuracy of aerial photogrammetric measurements depend on the total uncertainty (σ_T) associated with the determination of each shoreline position, which was sorted out by using the following relation [49]:

$$\sigma_T = \sqrt{\sigma_d^2 + \sigma_p^2 + \sigma_r^2 + \sigma_{co}^2 + \sigma_{wr}^2 + \sigma_{td}^2} \quad (1)$$

Such total uncertainty depends on documents own characteristics and digitalizing process [50], i.e., the digitalizing error (σ_d), accuracy linked to pixel size (σ_p), ortho-rectification error (σ_r), image co-registration error (σ_{co}), and on shoreline definition and position determination. In fact, shoreline is usually taken as the water/land contact, especially in microtidal environments [51–54] or as the seaward vegetation limit, dune foot, or cliff top, in mesotidal environments [10,55,56]. Given the micro-tidal nature of the studied coast and the absence of foredune ridges in most part of the zone, in this work, the shoreline position was defined as “the water line at the time of the photo” [53,54] and corrections were carried out according to wave run-up (σ_{wr}) and tidal conditions (σ_{td}) in the sense of Manno et al. [49]. Both parameters were calculated for the five areas in which the investigated littoral was divided. Calculated values of mentioned errors/uncertainties per each shoreline are presented in Table A2.

Evolution rates were calculated for the whole considered period and all the investigated shorelines, following the (previously described) WLR method and divided into seven classes (Table 2). The choice of intervals was based on the results obtained by means of the statistical analysis of the WLR data obtained with DSAS. It was considered that the 50% of the total data corresponded to “Moderate accretion”/“Moderate erosion” classes; values up to the 95% of the total data corresponded to “High accretion”/“High erosion” classes; and values >95% of the total data corresponded to “Very high accretion”/“Very high erosion” classes. It was decided to use the ± 0.2 interval as “Stability class” because it corresponds to the most frequent small changes related to seasonal oscillations (Table A3).

The “R” Project for Statistical Computing (<http://www.r-project.org/>) was used to create interaction plots to describe evolution classes distribution according to their location in areas free of structures and in correspondence of (or close to) coastal protection structures (revetments/seawalls, breakwaters and groins) and ports.

Finally, the analysis of the distribution of accretion/erosion/stability classes in relation to ports and rigid structures location allowed to determine drift- and swash-aligned coastal sectors and main direction of longshore transport.

Table 2. Definition of beach evolution classes.

Class	Beach State	m/year
1	Very high accretion	$\geq +1.5$
2	High accretion	$\geq +0.5; < +1.5$
3	Moderate accretion	$\geq +0.2; < +0.5$
4	Stability	$> -0.2; < +0.2$
5	Moderate erosion	$> -0.5; \leq -0.2$
6	High erosion	$> -1.5; \leq -0.5$
7	Very high erosion	≤ -1.5

4. Results

Within each unit, the most represented evolution class was considered as representative, as shown in Figure 2. A balance among eroded, accreted and stable beach areas was also calculated within each unit: at all cases (but 5) the unit balance coincided with the most represented evolution class (Table A3). None of the 47 units showed “Very high accretion” and only one unit (i.e., no. 37) presented “Very high erosion”. Specifically, 9 units, corresponding to 2854 transects (or 70.35 km), recorded accretion; 19 units, i.e., 3647 transects (or 89.9 km), stability; and 19 units, i.e., 4993 transects (or 124.07 km), erosion (Figure 2).

Taking into account the length inhomogeneity of the units, the balance was calculated between erosion, accretion and stability areas at each unit, and also at a global scale after considering all transects investigated. A total of 17 units had a positive balance (34,873.5 m²/year) and 28 a negative one (−64,611.9 m²/year). Overall, the investigated coast showed a negative net balance corresponding to the loss of 1784.30 km² of beach surface in the 1956–2016 period.

The distribution of the different classes of accretion, erosion and stability is presented in Figure 2. Two large erosion zones are evident along the SW area of Málaga Province and east of Almería Province (Figure 2). A large zone constituted by four “High accretion class” units was recorded at the eastern end of Málaga Province located between two areas of “Stability class”, one close to Torremolinos, and the other to La Herradura.

Concerning **accretion classes**, an example was observed east of Málaga (Units 18–21, Figure 2); as a result of the emplacement of several defence structures and nourishment works, a 31.1 km in length accretion coast was generated. At the unit close to Málaga (Unit 18, Figures 2 and 3), the most frequent evolution class observed was “High accretion”.

Among all the studied units, only two showed “Moderate accretion” and it was strictly related to the emplacement of structures. One example of this case is the area close to La Mamola (Unit 31, Figure 4): at the western edge of the unit, the beach is currently protected by six groins. Previously, there were eight shorter groins; three of them were removed and the easternmost structure was emplaced between 2001 and 2010 (Figure 4).

Erosion classes were mostly observed in the westernmost end of Málaga Province (between Units 4 and 10, Figure 2), close to the ports of La Duquesa, Estepona, and Puerto Banús, and a large number of coastal structures.

A similar trend was observed at Almerimar unit (Unit 37, Figures 2 and 5) where approximately 32 km² of beach surface were eroded during the 1956–2016 period. Coastal evolution of this unit was greatly linked to the construction in 1978 of the port of Almerimar (Figure 5).

Erosion classes were also frequently observed at river deltas. The evolution of Adra area (Unit 34, Figure 2) is presented in Figure 6. “Very high” and “High erosion” classes were observed on the area between the old and the present delta, especially at a 400 m long sector on the east side of the current mouth of the Adra River (Figure 6) whose basin was greatly modified during last decades: the construction, west of the river delta, of the port of Adra, interrupted the sedimentary transport and a new delta front was originated due to the artificial deviation of the main river channel (Figure 6).

The area including San Pedro de Alcántara (Unit 9) and Coral Beach (Unit 10, Figures 2 and 7), is constituted by two adjacent coastal units separated by Puerto Banús Port. This is a good example of shoreline evolution under the influence of reduced river supplies and massive development of structures. The area shows the presence of four rivers and seven streams, a port, several coastal structures and a strong anthropic impact (Figure 1).

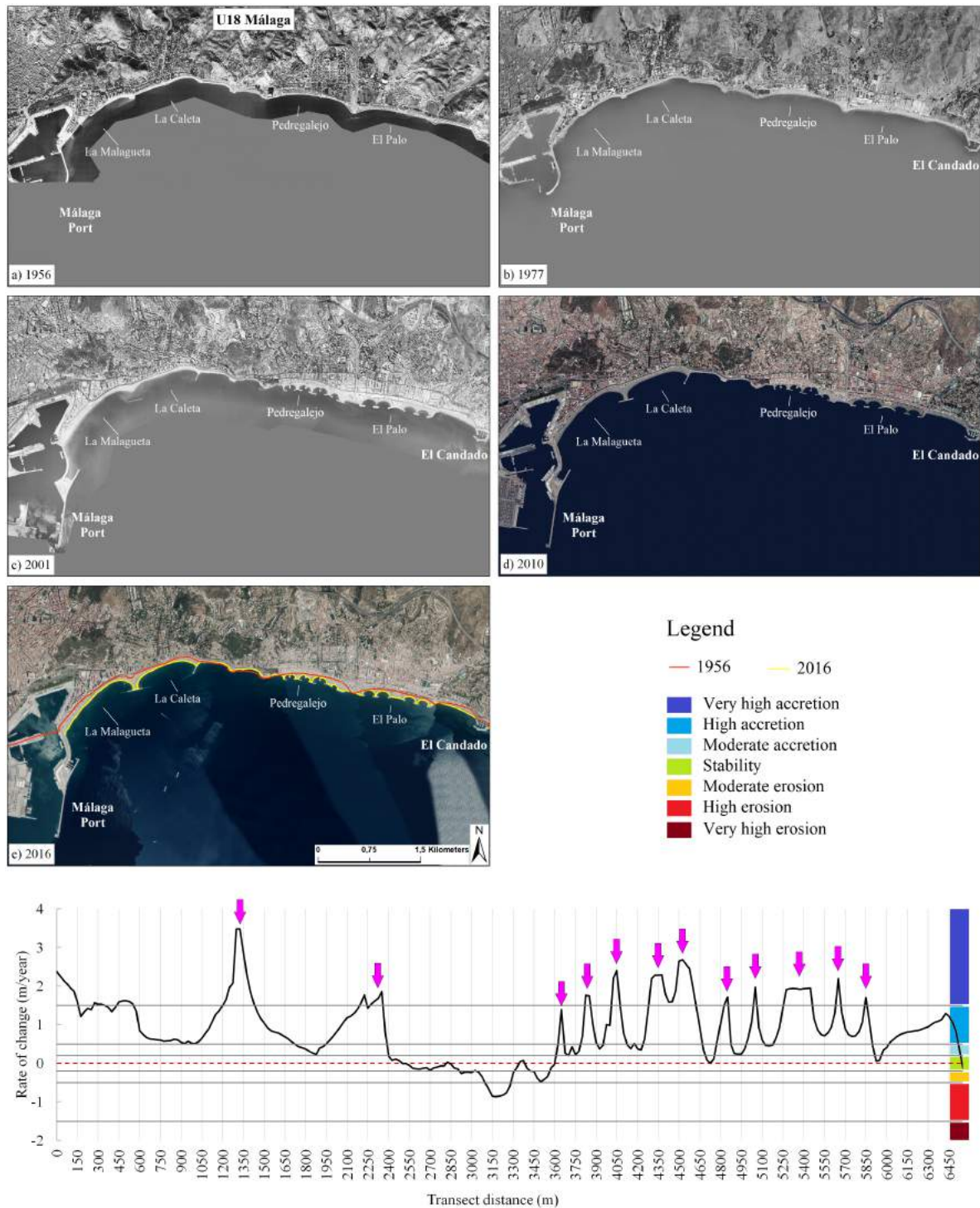


Figure 3. Evolution of Málaga area (Unit 18) from 1956 (a) to 2016 (e). “Moderate” to “Very high accretion” classes (Table A3) were recorded on the lee side of the breakwaters at La Malagueta Beach (up to +3.48 m/yr) and at La Caleta Beach (up to +1.86 m/yr), and in response to the structures emplaced at Pedregalejo and El Palo beaches (up to +2.68 m/yr). The first structure of Málaga Port was emplaced in 1588 and it was modified and enlarged several times, the last one in 1998. Arrows indicate the position of protection structures.

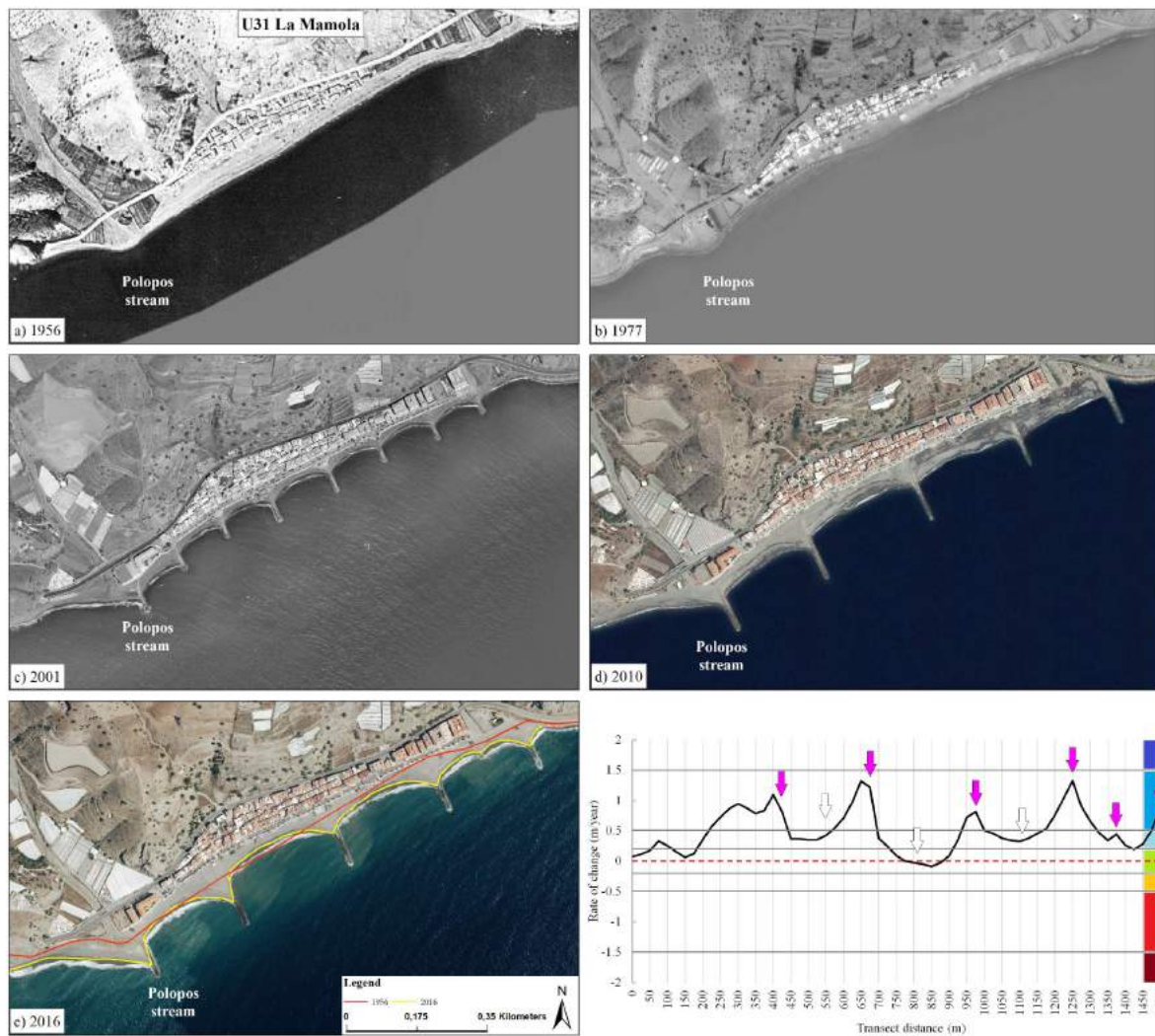


Figure 4. Evolution of La Mamola (Unit 31) from 1956 (a) to 2016 (e). “Moderate accretion” class represents 29.0% of the unit, corresponding to 1.05 km (Table A3) and the net beach surface evolution for the 1956–2016 period was positive (19,230 m², i.e., 320.50 m²/yr). In 1977, great erosion was observed east of the Polopos Stream mouth. In the 2001 aerial orthophoto, eight protection structures that did not solve erosion problems can already be observed. In the following years, such structures were modified and new ones were employed. Colored arrows indicate the position of present structures and white arrows those of previous ones.

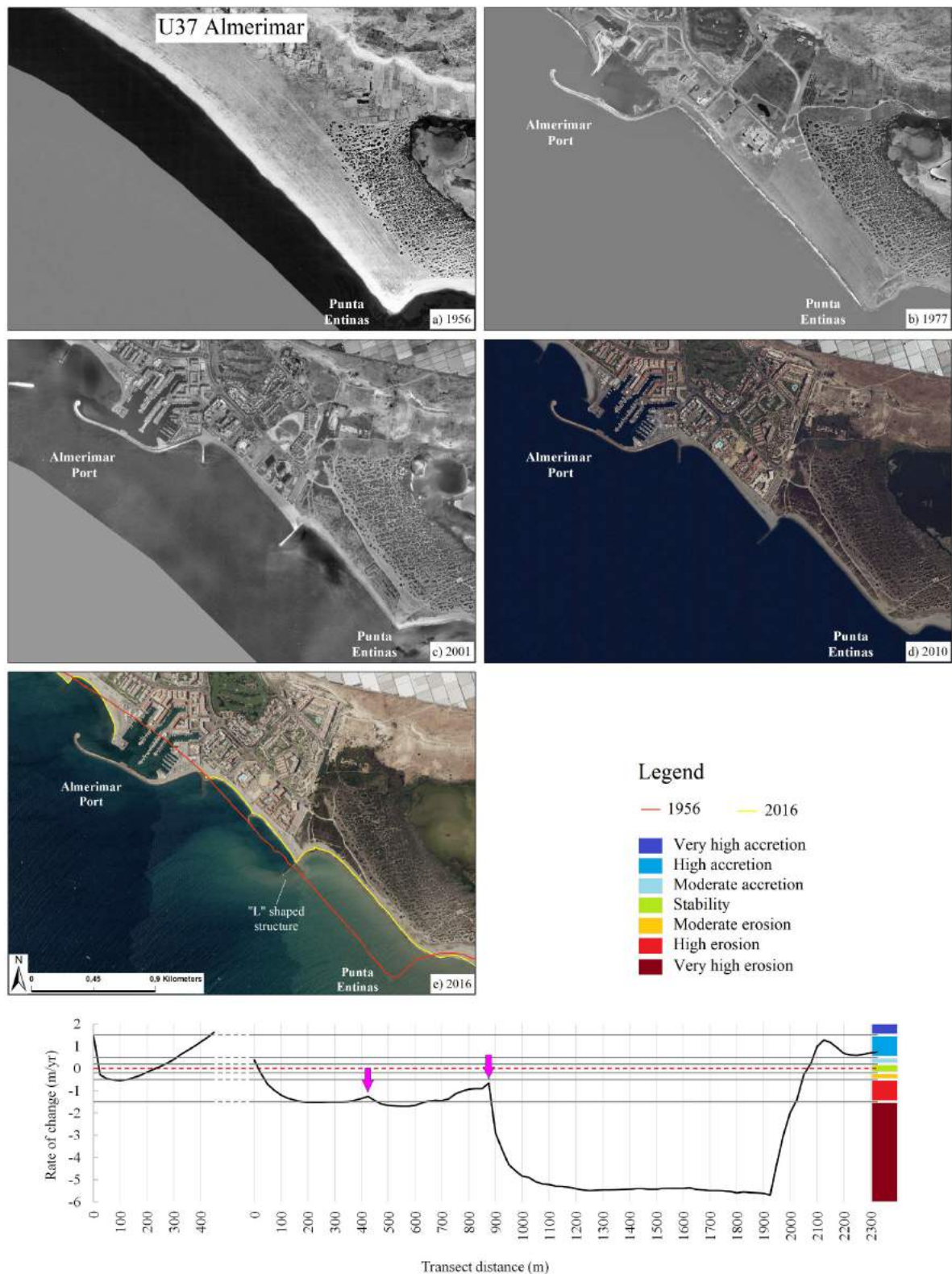


Figure 5. Evolution of Almerimar (Unit 37) from 1956 (a) to 2016 (e). It is the only unit that showed “Very high erosion” (63.8%, or 1.5 km) and the net beach surface evolution for the 1956–2016 period was negative (382,815 m², i.e., 6380.25 m²/yr). At the urbanized area situated between the port and the “L” shaped breakwater, erosion rates ranged between “High” and “Very high erosion” east of the port and of the “L”-shaped structure. Arrows indicate the position of protection structures.

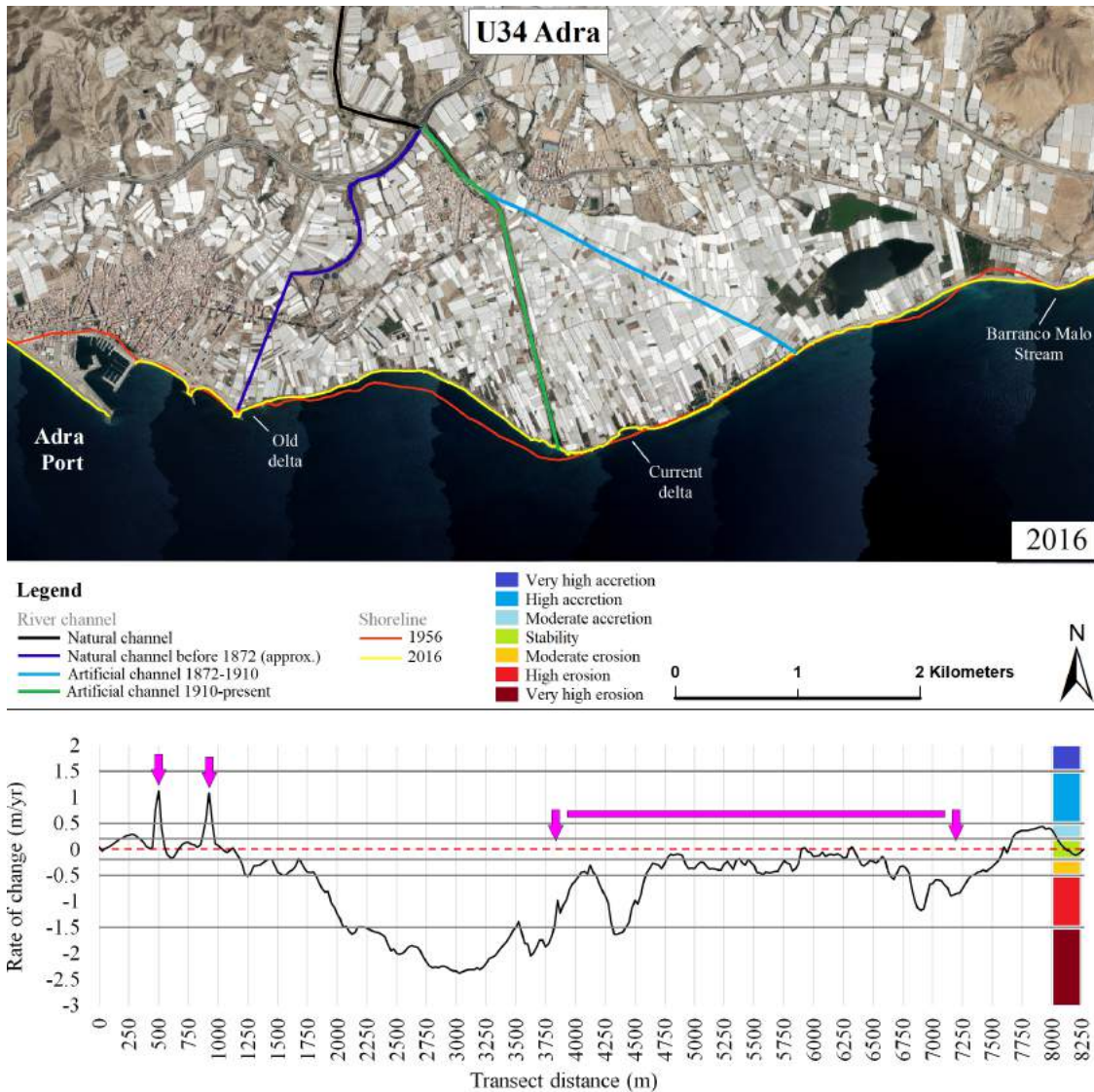


Figure 6. Delta of the Adra River (Unit 34) with the evolution of the main river channels [57]. The main (i.e., western) dock of the port was constructed in 1947. This unit prevalently recorded “Moderate erosion” (28%, or 2.32 km) and a negative beach surface balance since 258,315 m² (or −4305.25 m²/yr) were lost in the 1956–2016 period. “Accretion class” were observed in correspondence of the breakwaters (up to 1.12 m/yr) emplaced east of the port and in the easternmost part of the unit (up to 0.44 m/yr). Arrows indicate the position of protection structures and the continuous line the area where 100 small groins are located.

At San Pedro de Alcántara, erosion zones were located at western side of coastal structures and promontories and in correspondence of some rivers mouths, especially at Guadaiza River. Accumulation was observed east of Puerto Banús Port: this produced erosion at Nueva Andalucía Beach where breakwaters were emplaced forming tombolos that favored the migration of erosion problems at nearby areas, i.e., at Guadaiza River mouth, an area already eroding because of the decrease of river sediment supplies. In the 1970s, the emplacement of eight structures at Nueva Andalucía, favored accretion values up to 1.34 m/year (Figure 7).

At Coral Beach, “High erosion” was observed close to the mouth of the Verde River and the sector eastern of the port showed “High” and “Moderate accretion” values (Figure 7). A coastal structure, indicated with an arrow in Figure 7b,c), was built between 1956 and 1977 and retired between 2004 and 2006.

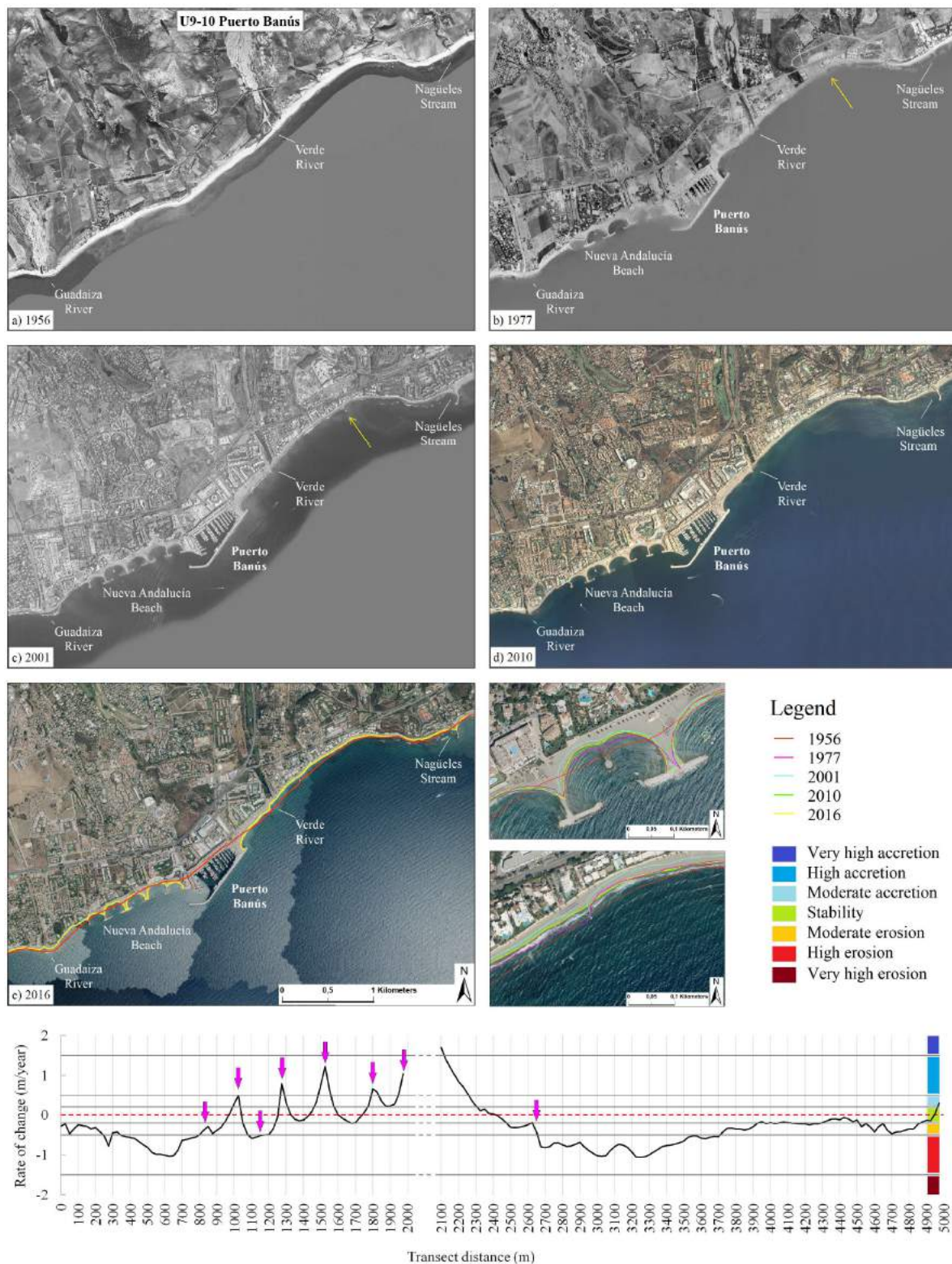


Figure 7. Evolution of Puerto Banús (Units 9 and 10) from 1956 (a) to 2016 (e). The port named Puerto Banús was constructed in 1970. Concerning units evolution, San Pedro de Alcántara (Unit 9), 10.25 km in length, and the adjacent Coral Beach (Unit 10), 2.9 km of length, are limited to the SW by Guadalmansa River and to the NE by the groin at the mouth of Nagüeles Stream. The most frequent class was “Moderate erosion” for Unit 9 (45.5%, i.e., 4.7 km) and “High erosion” for Unit 10 (36.2%, i.e., 1.05 km). Beach surface evolution recorded a negative trend at both units, i.e., $-1533.6 \text{ m}^2/\text{yr}$ for Unit 9 and $-579.75 \text{ m}^2/\text{yr}$ for Unit 10. Examples of coastal trend changes are also presented. Arrows indicate the position of protection structures.

Stability classes were observed at several pocket beaches (especially between Málaga and Granada provinces) and at few areas stabilized by coastal protection structures (e.g., La Línea de la Concepción).

La Herradura (Unit 24, Figure 8) represents a stable pocket beach that presented light accretion in its eastern edge, close to Punta de la Mona headland.

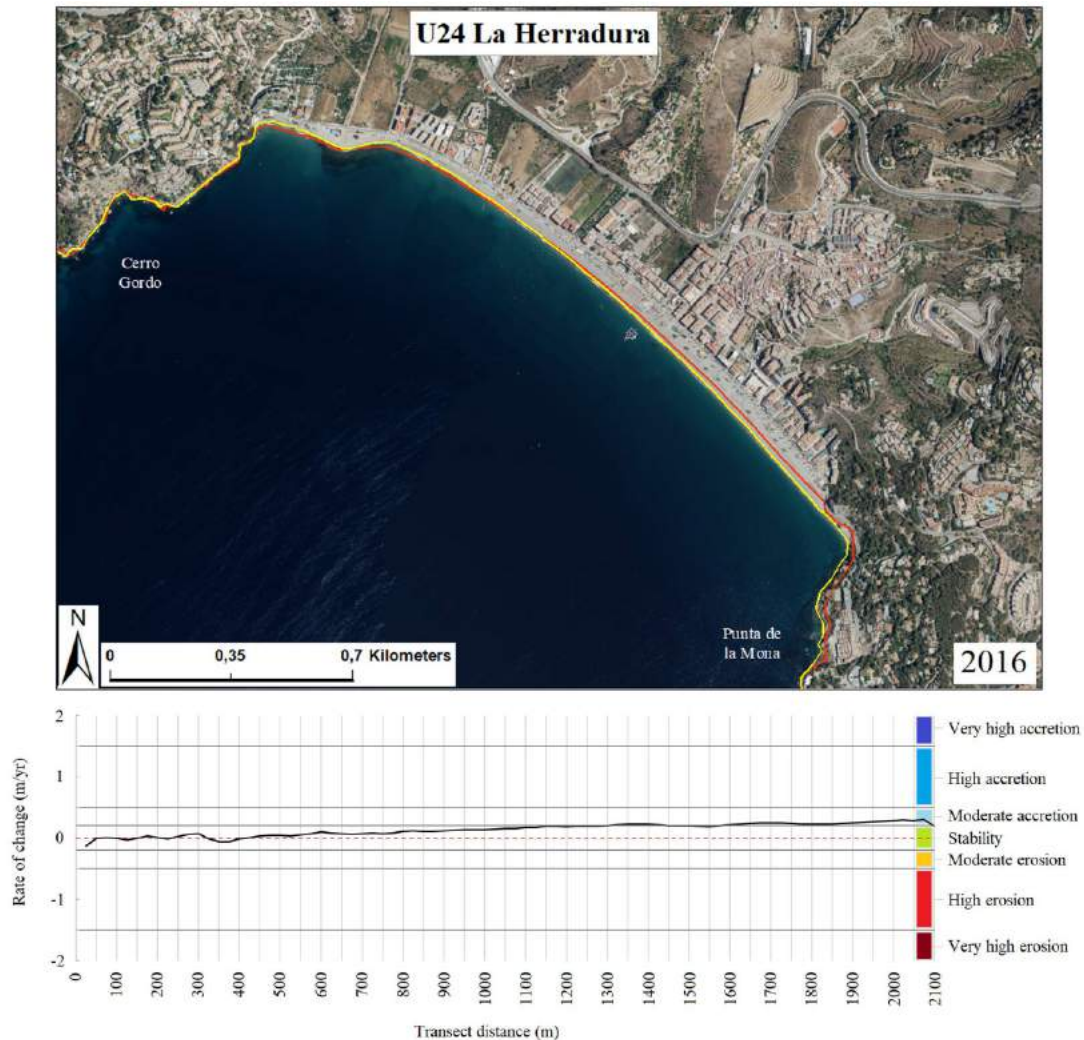


Figure 8. Evolution of La Herradura Beach (Unit 24). About 2 km in length, this beach is limited by two large rocky headlands, i.e., Cerro Gordo on the west, and Punta de la Mona on the east side. The most frequent class was “Stability” (70.2%, i.e., 1.4 km) and the net beach surface evolution was positive ($24.25 \text{ m}^2/\text{yr}$).

La Línea de la Concepción (Unit 1, Figures 2 and 9) is about 2.3 km in length. It is a very urbanized unit that counts with a promenade along the entire beach and several short groins.

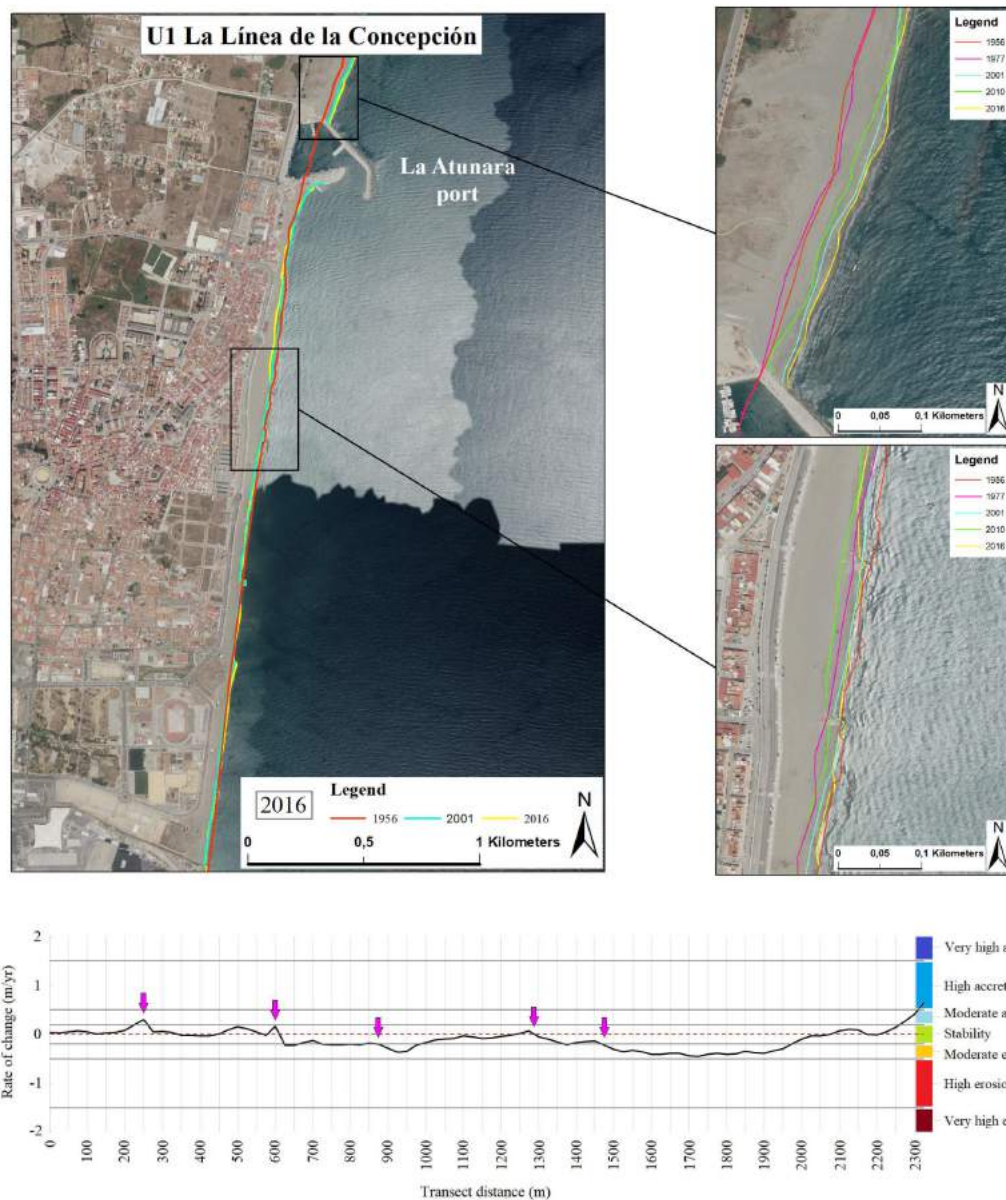


Figure 9. Evolution of La Línea de la Concepción (Unit 1). At this unit the most frequent class was “Stability” (60.6%, i.e., 1.4 km) and beach surface evolution was negative ($-97.75 \text{ m}^2/\text{yr}$). Accretion was observed in the southernmost part of the unit close to a small groin (up to 0.3 m/yr), and of the port (0.64 m/yr), which was constructed in 1994. “Moderate erosion” was observed at the central area of the unit (-0.37 m/yr) and up-drift of the easternmost groin (-0.46 m/yr). Examples of coastal trend changes are also presented. Arrows indicate the position of protection structures.

5. Discussion

This section discusses the distribution of erosion/accretion/stability classes (or evolution classes) according to their location, i.e., up-drift, down-drift or in correspondence of coastal structures, or in “natural” areas free of structures. Then, the distribution of evolution classes was analyzed considering structures location/characteristics and wave approaching front directions to determine the distribution of swash- and drift-aligned costal sectors and prevalent longshore transport direction.

5.1. Evolution Classes at Natural Coastal Sectors

Transects located at natural areas (Figure 10a), i.e., areas with no ports and protection structures, recorded average retreat rates of 0.17 m/year . Special attention was devoted to the behavior of

transects located at deltas and river mouths (Figure 10a), which showed average retreat rates of 0.62 m/year, reaching high and very high erosion values, e.g., 1.88 m/year at Adra Delta, 1.00 m/year at Andarax Delta and 1.15 m/year at Aguas River mouth, in Almería Province. Retreat rates of 3.71 and 0.82 m/year were, respectively, recorded at Vélez River Delta and at Verde River mouth in Málaga Province.

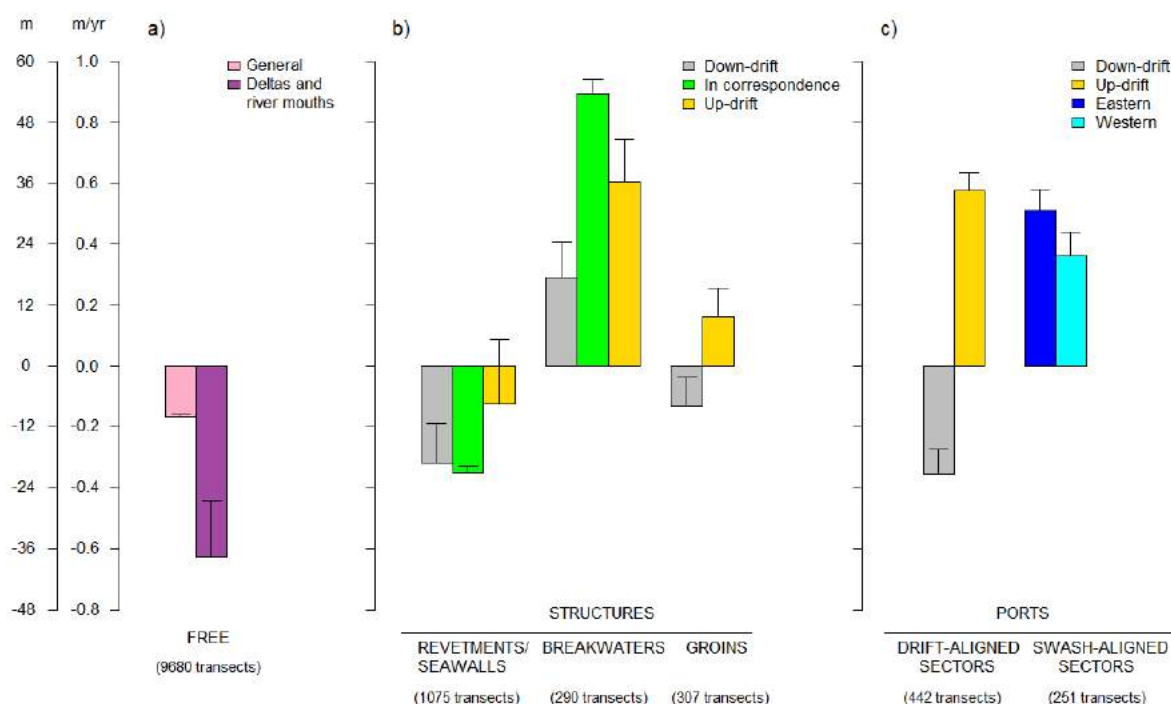


Figure 10. Interaction plots giving evolution values and trends of transects at: (i) free areas, distinguishing between transects located at any general place and in correspondence of rivers and deltas (a); (ii) transects located up- and down-drift or in correspondence of seawalls/revetments, breakwaters and groins (b); and (iii) at up- and down-side of ports in drift-aligned coastal sectors and eastern or western side of ports in swash-aligned coastal sectors (c) (Figure 2).

In Almería, the erosive evolution of the deltas of Andarax and Adra rivers, and of the eastern zone of the province, were greatly influenced by the torrential nature of those rivers and other streams, as well as by the progressive construction of dams that greatly reduced sediment inputs to the littoral [58,59], a common trend also observed at other places by Syvitski et al. [60] and Kim et al. [61]. The Beninar Dam, built in 1988 in the Adra River, brought to the construction of about 100 small groins along the east side of the current delta [39].

The Vélez River delta is a good example of an erosive behavior. The delta apex is very susceptible to erosion: a divergence of transport was observed at such location and sediments were accumulated at both sides of the apex [39], this being a common trend also observed at the Guadalfeo and Andarax deltas [39], as well as on the Nile [62,63], Ebro [11] and the Arno [64] deltas. Since 1988, several dams were placed in the basin of the Vélez River that significantly reduced fluvial sedimentary load [65]. Accretion was observed at the eastern area of the delta because of the emplacement of coastal structures and periodic nourishment works [39,66,67].

Located on the Verde River, La Concepción Dam is the most important fluvial engineering work of Costa del Sol [68], with an artificial lake surface of 2.14 km², a volume capacity of 57×10^6 m³ and an affected river length of 5 km. Before dam construction, the Verde River constituted the main source of sediment to the Marbella coastal area [68–70].

Transects located at pocket beaches showed the prevalence of stability values and a typical pivoting behavior [71], e.g., La Herradura (Unit 24, Figure 8). This is because pocket beaches are

restricted sedimentary systems, i.e., they experience little or no connection to other systems because the presence of rocky headlands limiting them [72].

5.2. Evolution Classes versus Coastal Structures Location and Characteristics

In sandy sectors, the spatial distribution of accretion, erosion and stability areas is essentially influenced by the emplacement of protection structures, ports and existing natural headlands and the way such structures interact with the incoming waves, as observed at different areas by the authors of [31,34,73–75].

Concerning the effect of coastal protection structures, seawalls and revetments reflect wave energy; this process restricts the natural inland migration of sediments and, consequently, induces erosion and beach losses in front of them [76,77], as also observed in this paper. Specifically, 1075 transects were linked to the presence of revetments and seawalls and, even though they were located in correspondence, up- or down-drift of structures, they were always characterized by high erosion values (from 0.13 to 0.35 m/year, Figure 10b).

Breakwaters produce tombolos [78,79], as widely observed at Málaga Province (e.g., Málaga and Puerto Banús, Figures 3 and 7) at these areas accretion classes were recorded, especially where structures were very numerous. Specifically, 290 transects were located in correspondence and up- or down-drift of breakwaters. This typology of structure was much more effective in retaining sediments than groins and showed average accretion values up to 0.89 m/year, close to the ones recorded up-drift of ports (Figure 10b,c).

Shore-normal structures (i.e., groins and jetties) and ports act as absolute or permeable cell limits [73] that affect surf zone circulation usually producing accretion up-drift and erosion down-drift, as extensively observed by Anfuso et al. [34] along the Caribbean coast of Colombia or by Anfuso et al. [80] in southeastern Sicily. This was also recorded in this paper: transects located close to groins clearly reflected longshore transport effect, i.e., up-drift accretion with average values of 0.16 m/year and average down-drift values of 0.13 m/year (Figure 10b).

Concerning transects located close to ports, they were divided into two groups, i.e., up- and down-drift transects when ports were located in drift-aligned coastal sectors (i.e., in a coastal area where a clear longshore transport direction was observed; see Figure 2 and Section 5.3) and in eastern and western transects when they are close to ports located in swash-aligned sectors (see Figure 2 and Section 5.3).

Regarding ports located in drift-aligned areas, transects located up-drift recorded the greatest accretion classes respect to other typologies of structures and erosive transects were observed in down-drift areas (Figure 10c), e.g., at Sotogrande Port in Cádiz Province and at Garrucha Port in Almería, a common trend observed along sandy coasts [77,79]. Ports located in swash-aligned sectors showed accretion at both sides (Figure 10c). The form and dimensions of the newly formed beaches depend on the characteristics of the structures and wave regime as observed by different authors (e.g., [31,34,73]).

Commonly, the development of erosion processes in down-drift areas was prevented with the progressive emplacement of new structures generating the so called “domino” effect [81]. This process, frequently observed along the Mediterranean coast [31,34,38,80], translates and amplifies erosion processes in down-drift areas. An example was the construction of the port of Almerimar (Figure 5) in 1978; according to [59], it caused the down-drift disappearance of 20,000 m² of beach surface. In 1996, two structures were successively emplaced to reduce coastal erosion; these structures proved to be ineffective and caused the loss of more than 135,500 m² [59]. Nowadays, periodic artificial nourishments are carried out to maintain this beach. Despite the emplacement of structures, an important cause of beach erosion during the 1956–1988 period was the illegal extraction of more than 5 million cubic meters of sand from beaches and dunes in Punta Entinas–Sabinar zone [59].

Last, shoreline evolution was not always uniform, i.e., recorded an inversion of trend, usually from erosion to accretion, as observed at several erosion spots where the erosive trend was contrasted

by the emplacement of coastal structures and/or artificial nourishments, e.g., at Puerto Banús (Figure 7) and at La Línea de la Concepción (Figure 9).

5.3. Swash- and Drift-Aligned Coastal Sectors

The analysis of beach plan form and its temporal variation, which depends on wave climate [75,82] and natural and human structures characteristics [73], can be used to determine coastal sectors with drift-aligned or swash-aligned shoreline trends. Drift-aligned shoreline sectors are the result of a clear unidirectional transport while swash-aligned shoreline sectors are the result of a bidirectional longshore transport and/or a cross-shore transport [31].

Swash-aligned shoreline form was observed at two extended areas: at Costa del Sol (Málaga) and in the Gulf of Almería (Figure 2). The former (Málaga, Unit 18) is shown in Figure 3: this is a strongly urbanized coast [31,66], with a large number of coastal protection structures. Huge amounts of sediments, which altered the natural dynamics of the area, were injected to counteract erosion processes linked to recurrent storms. Further alteration to the dynamic characteristics of this area was caused by the construction of many groins, successively replaced by breakwaters, which favored the creation of tombolos [66] and the formation of a stable, swash-aligned coast [31].

Concerning the main transport directions observed in this paper (Figure 2), they reflected wave roses (Figure 1) and storms approaching directions presented by Molina et al. [42]. The drift-aligned, easternmost part of the investigated littoral is sheltered, because of its geographic location, to the Atlantic swell waves and exposed to east approaching fronts forming an angle of ca. 45 degrees with the shoreline; the main sediment transport direction observed at this area confirmed such data showing a NE-SW main transport trend at La Línea de la Concepción (Unit 1, Figure 9) and at Sotogrande where the port, constructed in 1987, clearly interrupted longshore transport (Figure 11a).



Figure 11. Examples of drift-and swash-aligned shoreline sectors. Stogrande Port (a) was constructed in 1987, Adra Port (b) in 1947 (the first emplacement) and the construction of Garrucha Port (c) started in 1931 and the last modification was carried out in 2009.

At the central part of the studied coast (Points 2 and 3, Figure 1), which is drift-aligned, wind and waves approached from W, E and E-NE directions, the W component prevailing due to the increase of the western geographic fetch. Hence, offshore wave fronts are broadly normal to the coast and the most energetic events approached from these directions too [42].

As observed in Suffolk (UK) by Burningham and French [83], the bimodal wave climate has a strong control on sediment movement alongshore. The W-E transport direction was observed in the central part of the investigated littoral, e.g., at Adra (Unit 34, Figures 6 and 11b) with a clear evidence at Adra Port where a dock was built in 1947 to avoid infilling problems [58]. The eastern coast of the studied area, which is drift-aligned, is NNE-SSW oriented so it is sheltered to the W, and the E-NE approaching directions prevail (forming an angle of ca. 30 degrees with the shoreline, Point 4, Figure 1); this is confirmed by the NE-SW transport direction observed in this study, e.g., at Garrucha (Unit 47, Figure 11c).

6. Conclusions

This study analyzed the evolution, during a 60-year time span, of the Mediterranean coast of Andalusia, making special emphasis on the impact of coastal structures. The coast was divided into 47 units of different lengths and, within each unit, the evolution rates were calculated by using the DSAS extension of ArcGIS software. Along the investigated area, 9 units recorded accretion, 19 recorded stability and 19 erosion. Seventeen units presented a positive balance and 28 units a negative one. The investigated littoral showed a negative net balance of 29,738.4 m²/year corresponding to the loss of 1784.30 km² of beach surface in the 1956–2016 period.

Concerning the influence of coastal structures, it was observed as accretion areas were essentially observed up-drift of ports and groins and in correspondence of breakwaters. Coastal areas in front of revetments always recorded erosion, which was also relevant down-drift of ports and groins, as well as at the mouths of largest rivers and deltas. Stability was observed at several pocket beaches and at areas stabilized by coastal protection structures. The analysis of shoreline trend and form as well as the influence of coastal protection structures and ports in promoting erosion or accretion processes, allowed to reconstruct the distribution of drift- and swash-aligned coastal sectors and longshore transport directions, mainly depending on coastal orientation with respect to the prevailing wave approaching fronts. This is a quite complex, indented coast associated with an active alpine orogen contacting the sea, affected by two prevailing winds blowing parallel to the main direction of the coast. As a result, swash-aligned coastal sectors predominate inside the main embayments (e.g., Málaga Bay and Almería Gulf), while the rest is represented by drift-aligned sectors. Nevertheless, the direction and sense of prevailing drift currents change from one sector to another, e.g., southwards in the NE-SW oriented sectors, eastwards in the central sectors.

Author Contributions: Data curation, R.M. and G.M.; Formal analysis, R.M., G.M. and G.A.; Methodology, R.M., G.M., G.A. and F.J.G.P.; Software, R.M., G.M. and G.A.; Supervision, G.A. and F.J.G.P.; Writing—original draft, R.M., G.M., G.A. and F.J.G.P.; Writing—review & editing, G.A., F.J.G.P. and G.M.

Funding: This research received no external funding.

Acknowledgments: This work is a contribution to the Andalusia P.A.I. Research Group no. RNM-328 and has been partially developed at the Centro Andaluz de Ciencia y Tecnología Marinas (CACYTMAR), Puerto Real (Cádiz, Spain).

Conflicts of Interest: The authors declare no conflict of interest.

Appendix A

Table A1. Characteristics of the studied units. * Cardinal points indicate the location of the Harbour/Port.

ID	Coastal Name	Morphology	Number of the Defence Structures			Close to Harbour/Port (*)
			Groins	Breakwaters	Revetments	
1	La Línea de la Concepción	Straight coast	7	–	–	Yes (N)
2	El Zabal	Straight coast	–	–	–	Yes (S)
3	Torreguadiaro	Straight coast and Pocket beach	3	–	–	Yes
4	La Chullera	Straight coast	1	–	1	Yes (N)
5	San Luis de Sabinillas	Straight coast	–	–	–	Yes (S)
6	La Gaspara	Straight coast and Pocket beach	2	–	3	Yes
7	Estepona	Straight coast	2	1	–	Yes (N)
8	Guadalmansa (S)	Straight coast	1	–	1	No
9	San Pedro de Alcántara	Straight coast	11	5	1	No (SW); Yes (NW)
10	Coral Beach (Puerto Banús \$N4)	Pocket beach	1	–	–	Yes (SW)
11	Marbella (W)	Straight coast	2	1	–	Yes (NW)
12	Marbella (E)	Pocket beach and Straight coast	12	–	–	Yes (W)
13	Mijas	Straight coast	–	–	–	Yes (W)
14	Fuengirola (S)	Straight coast	2	1	1	Yes
15	Benalmádena	Straight coast	6	2	2	Yes (NE)
16	Torremolinos	Straight coast	–	–	2	Yes (SW)
17	Málaga (S)	Straight coast	1	–	–	Yes (NE)
18	Málaga (E)	Straight coast	1	13	2	Yes (W and E)
19	La Cala del Moral	Pocket beach	1	1	1	No
20	Rincón de La Victoria	Straight coast	–	–	5	No
21	Torre del Mar	Straight coast	10	2	2	Yes
22	Caleta de Vélez	Straight coast	1	–	5	No
23	Nerja	Pocket beach	–	–	1	No
24	La Herradura	Pocket beach	–	–	–	No
25	Almuñécar	Pocket beach	–	–	–	No
26	Velilla Tamaray	Pocket beach	3	1	1	No
27	Salobreña	Straight coast	2	–	–	Yes (E)
28	Torrenueva	Pocket beach	4	4	–	Yes (W)
29	Carchuna	Straight coast	–	–	–	No
30	Castel de Ferro	Pocket beach	–	4	–	No
31	La Mamola	Straight coast	5	–	2	No
32	Albuñol	Straight coast	2	–	1	No
33	Adra (E)	Straight coast	8	–	–	Yes (E)
34	Adra (W)	Straight coast	88	2	9	Yes (W)
35	Balerma	Straight coast	8	–	–	No
36	Ensenada de San Miguel	Pocket beach	1	–	–	Yes (E)
37	Almerimar	Pocket beach	3	1	–	Yes (NW)
38	San Agustín	Straight coast	–	–	–	No
39	Roquetas de Mar (S)	Straight coast	2	–	1	Yes (N)
40	Roquetas de Mar (N)	Straight coast	–	1	–	Yes (N and S)
41	Almería	Straight coast	4	1	–	Yes (W)
42	Costacabana	Straight coast	6	–	–	No
43	Cabo de Gata	Straight coast	–	–	–	No
44	Playa de los Genoveses	Pocket beach	–	–	–	No
45	Carboneras	Pocket beach	–	–	–	Yes
46	La Parata	Straight coast	–	–	–	No
47	Garrucha	Straight coast	3	2	–	Yes (S)

Table A2. Shoreline determination error for each document used (Equation (1)).

Year	Error Components (m)						
	σ_d	σ_p	σ_r	σ_{co}	σ_{wr}	σ_{td}	σ_T
Area 1 (1–12 units)							
1956	7.60	1.00	4.00	0.50	2.60	11.70	14.80
1977	2.10	0.50	3.30	0.50	2.60	11.70	12.60
2001	2.10	0.50	1.00	1.00	2.60	11.70	12.30
2010	1.90	0.50	0.50	0.00	2.60	11.70	12.10
2016	0.70	0.25	0.50	0.00	2.60	11.70	12.00
Area 2 (13–23 units)							
1956	7.60	1.00	4.00	0.50	2.80	7.20	11.60
1977	2.10	0.50	3.30	0.50	2.80	7.20	8.70
2001	2.10	0.50	1.00	1.00	2.80	7.20	8.20
2010	1.90	0.50	0.50	0.00	2.80	7.20	8.00
2016	0.70	0.25	0.50	0.00	2.80	7.20	7.80
Area 3 (24–37 units)							
1956	7.60	1.00	4.00	0.50	3.20	4.30	10.20
1977	2.10	0.50	3.30	0.50	3.20	4.30	6.70
2001	2.10	0.50	1.00	1.00	3.20	4.30	5.90
2010	1.90	0.50	0.50	0.00	3.20	4.30	5.70
2016	0.70	0.25	0.50	0.00	3.20	4.30	5.40
Area 4 (38–43 units)							
1956	7.6	1.00	4.00	0.50	3.10	2.80	9.60
1977	2.10	0.50	3.30	0.50	3.10	2.80	5.80
2001	2.10	0.50	1.00	1.00	3.10	2.80	4.90
2010	1.90	0.50	0.50	0.00	3.10	2.80	4.60
2016	0.70	0.25	0.50	0.00	3.10	2.80	4.30
Area 5 (44–47 units)							
1956	7.60	1.00	4.00	0.50	3.30	1.40	9.40
1977	2.10	0.50	3.30	0.50	3.30	1.40	5.40
2001	2.10	0.50	1.00	1.00	3.30	1.40	4.40
2010	1.90	0.50	0.50	0.00	3.30	1.40	4.10
2016	0.70	0.25	0.50	0.00	3.30	1.40	3.70

Table A3. Results of coastal evolution during the 1956–2016 period. Blue numbers indicate the most frequent class. * Unit net balance: A, accretion; E, erosion.

Unit	Name	Accretion (%)			Stability (%)	Erosion (%)			Unit Net Balance *	Longitude (km)	Morphology
		Very High	High	Moderate	Moderate	High	Very High				
1	La Línea de la Concepción	0.0	1.1	3.2	60.6	35.1	0.0	0.0	E	2.3	
2	El Zabal	0.0	53.2	36.2	10.6	0.0	0.0	0.0	A	7.5	
3	Torreguadiaro	0.0	1.2	9.0	25.3	20.4	21.6	22.4	E	6.0	
4	La Chullera	0.0	0.5	1.0	16.7	41.4	39.9	0.5	E	5.0	
5	San Luis de Sabinillas	0.8	1.7	5.9	22.9	25.4	43.2	0.0	E	2.9	
6	La Gaspara	0.0	0.0	0.0	0.9	15.1	83.9	0.0	E	5.4	Drift aligned
7	Estepona	5.5	28.6	14.3	50.5	1.1	0.0	0.0	A	2.2	NE-SW
8	Guadalmansa (S)	0.0	0.0	0.0	45.9	50.0	4.1	0.0	E	7.3	
9	San Pedro de Alcántara	0.0	4.4	4.9	14.6	45.5	30.7	0.0	E	10.2	
10	Coral Beach (Puerto Banús N)	0.9	5.2	2.6	20.7	34.5	36.2	0.0	E	2.9	
11	Marbella (W)	0.0	6.5	22.0	61.8	8.1	1.6	0.0	A	3.0	
12	Marbella (E)	0.6	5.8	2.7	26.6	31.4	32.9	0.0	E	12.8	
13	Mijas	0.0	7.0	5.7	49.4	20	14.5	3.5	E	10.0	
14	Fuengirola (S)	0.0	1.9	20.1	50	26.9	1.1	0.0	E	6.5	
15	Benalmádena	3.4	17.9	22.8	48.1	6.6	1.1	0.0	A	8.7	
16	Torremolinos	0.0	21.2	24.0	24.5	13.1	11.4	5.8	A	8.9	
17	Málaga (S)	2.1	2.1	2.6	23.7	9.8	53.1	6.7	E	4.8	Swash aligned
18	Málaga (E)	22.4	43.7	12.5	13.3	4.9	3.0	0.0	A	6.5	
19	La Cala del Moral	1.2	42.7	28.0	28.0	0.0	0.0	0.0	A	2.0	
20	Rincón de La Victoria	1.5	33.6	14.7	25.0	13.2	8.0	3.8	A	16.2	
21	Torre del Mar	0.0	31.0	24.0	17.1	11.2	8.9	7.8	A	6.4	
22	Caleta de Vélez	0.0	7.1	9.5	33.5	24.9	24.9	0.0	E	8.0	
23	Nerja	0.0	0.0	4.3	47.8	47	0.9	0.0	E	2.8	
24	La Herradura	0.0	0.0	29.8	70.2	0.0	0.0	0.0	A	2.1	
25	Almuñécar	0.0	2.3	14	83.7	0.0	0.0	0.0	A	1.0	
26	Velilla Tamaray	15.7	39.3	30.7	14.3	0.0	0.0	0.0	A	3.5	
27	Salobreña	22	14.4	8.0	9.8	11.0	23.1	11.7	A	6.6	
28	Torrenueva	3.4	22.8	15.9	23.4	6.2	28.3	0.0	A	3.6	
29	Carchuna	0.0	3.5	2.5	77.1	15.9	1.0	0.0	E	5.0	Drift aligned
30	Castel de Ferro	0.0	14.9	5.7	56.3	10.3	12.6	0.0	E	2.1	W-E
31	La Mamola	0.0	15.9	29.0	28.3	19.3	7.6	0.0	A	3.6	
32	Albuñol	16.2	12.7	6.4	24.5	36.8	3.4	0.0	E	5.1	
33	Adra (E)	0.0	0.6	12.5	78.8	8.1	0.0	0.0	A	4.0	
34	Adra (W)	0.0	1.5	6.9	24.1	28.0	19.0	20.5	E	8.3	
35	Balerna	0.0	0.0	0.9	75.8	22.7	0.6	0.0	E	8.4	
36	Ensenada de San Miguel	0.5	9.9	3.5	5.4	4.5	76.2	0.0	E	5.0	
37	Almerimar	0.0	10.6	1.1	1.1	2.1	21.3	63.8	E	2.3	
38	San Agustín	0.0	25.1	13.7	11.3	10.7	23.4	15.8	E	12.6	
39	Roquetas de Mar (S)	0.0	0.0	2.4	34.1	20.2	30.8	12.5	E	5.2	
40	Roquetas de Mar (N)	0.3	2.0	1.0	22.4	33.4	40.8	0.0	E	7.4	Swash aligned
41	Almería	1.0	14.1	11.5	23	15.3	35.1	0.0	E	7.8	
42	Costacabana	0.0	1.4	2.5	82.0	11.2	3.0	0.0	E	9.1	
43	Cabo de Gata	0.0	0.0	5.7	55.4	27.0	11.8	0.0	E	12.6	
44	Playa de los Genoveses	0.0	0.0	0.0	13.8	23.1	63.1	0.0	E	1.6	
45	Carboneras	9.0	11.2	2.2	6.0	34.3	37.3	0.0	E	3.3	Drift aligned
46	La Parata	1.5	7.5	6.0	3.6	52.4	28.9	0.0	E	8.6	NE-SW
47	Garrucha	2.7	5.7	29.7	24.3	3.8	13.3	20.5	E	7.0	

References

1. Brown, A.; McLachlan, A. Sandy shore ecosystems and the threats facing them: Some predictions for the year 2025. *Environ. Conserv.* **2002**, *29*, 62–77. [CrossRef]
2. Klein, Y.L.; Osleeb, J.P.; Viola, M.R. Tourism-generated earnings in the coastal zone: A regional analysis. *J. Coast. Res.* **2004**, *20*, 1080–1088.
3. UNWTO. *Tourism Highlights*; Technical Report; United Nations World Tourism Organization: Madrid, Spain, 2015.
4. Jones, A.; Phillips, M. *Disappearing Destinations: Climate Change and Future Challenges for Coastal Tourism*; CABI International: Wallingford, UK, 2011.
5. Bacon, S.; Carter, D.T. Wave climate changes in the North Atlantic and North Sea. *Int. J. Climatol.* **1991**, *11*, 545–558. [CrossRef]
6. Dupuis, H.; Michel, D.; Sottolichio, A. Wave climate evolution in the Bay of Biscay over two decades. *J. Mar. Syst.* **2006**, *63*, 105–114. [CrossRef]
7. Komar, P.D.; Allan, J.C. Increasing hurricane-generated wave heights along the US East Coast and their climate controls. *J. Coast. Res.* **2008**, *24*, 479–488. [CrossRef]
8. Soomere, T. *Extremes and Decadal Variations of the Northern Baltic Sea Wave Conditions*; Springer: Dordrecht, The Netherlands, 2008; pp. 139–157.
9. Crowell, M.; Leatherman, S.P.; Buckley, M.K. Historical shoreline change: Error analysis and mapping accuracy. *J. Coast. Res.* **1991**, *7*, 839–852.
10. Crowell, M.; Leatherman, S.P.; Buckley, M.K. Shoreline change rate analysis: Long term versus short term data. *Shore Beach* **1993**, *61*, 13–20.
11. Jiménez, J.A.; Sánchez-Arcilla, A. Medium-term coastal response at the Ebro delta, Spain. *Mar. Geol.* **1993**, *114*, 105–118. [CrossRef]
12. Gorman, L.; Morang, A.; Larson, R. Monitoring the coastal environment; part IV: Mapping, shoreline changes, and bathymetric analysis. *J. Coast. Res.* **1998**, *14*, 61–92.
13. El-Asmar, H.M. Short term coastal changes along Damietta-Port Said coast northeast of the Nile Delta, Egypt. *J. Coast. Res.* **2002**, *18*, 33–441.
14. Morton, R.A. Temporal and spatial variations in shoreline changes and their implications, examples from the Texas Gulf Coast. *J. Sediment. Res.* **1979**, *49*, 1101–1111.
15. Corbau, C.; Tessier, B.; Chamley, H. Seasonal evolution of shoreface and beach system morphology in a macrotidal environment, Dunkerque area, Northern France. *J. Coast. Res.* **1999**, *15*, 97–110.
16. Anfuso, G.; Gracia, F. Morphodynamic characteristics and short-term evolution of a coastal sector in SW Spain: Implications for coastal erosion management. *J. Coast. Res.* **2005**, *21*, 1139–1153. [CrossRef]
17. Anfuso, G.; Pranzini, E.; Vitale, G. An integrated approach to coastal erosion problems in northern Tuscany (Italy): Littoral morphological evolution and cell distribution. *Geomorphology* **2011**, *129*, 204–214. [CrossRef]
18. Romine, B.; Fletcher, C.; Genz, A.; Barbee, M.; Dyer, M.; Anderson, T.; Lim, S.; Vitousek, S.; Bochicchio, C.; Richmond, B. National Assessment of Shoreline Change: A GIS Compilation of Vector Shorelines and Associated Shoreline Change Data for the Sandy Shorelines of Kauai, Oahu and Maui, Hawaii. U.S. Geological Survey Open-File Report 2011-1009. Available online: <https://pubs.usgs.gov/of/2011/1009/> (accessed on 10 June 2019).
19. Rangel-Buitrago, N.G.; Anfuso, G.; Williams, A.T. Coastal erosion along the Caribbean coast of Colombia: Magnitudes, causes and management. *Ocean Coast. Manag.* **2015**, *114*, 129–144. [CrossRef]
20. Leatherman, S.P. Shoreline mapping: A comparison of techniques. *Shore Beach* **1983**, *51*, 28–33.
21. Houston, J. The economic value of beaches: A 2013 update. *Shore Beach* **2013**, *81*, 3–11.
22. Clark, J.R. *Coastal Zone Management Handbook*; CRC Press/Lewis Publishers: Boca Raton, FL, USA, 1996.
23. UNWTO. *Tourism Highlights*; Technical Report; United Nations World Tourism Organization: Madrid, Spain, 2006.
24. Dodds, R.; Kelman, I. How climate change is considered in sustainable tourism policies: A case of the Mediterranean islands of Malta and Mallorca. *Tour. Rev. Int.* **2008**, *12*, 57–70. [CrossRef]
25. Malvárez, G.C. The history of shoreline stabilization on the Spanish Costa del Sol. In *Pitfalls of Shoreline Stabilization*; Springer: Dordrecht, The Netherlands, 2012; pp. 235–249.

26. Martínez, J.M.R.; Padilla, Y.R.; Jurado, E.N. Atributos urbanos contemporáneos del litoral mediterráneo en la crisis global: Caso de la zona metropolitana de la Costa del Sol. *Scr. Nova Rev. Electrónica De Geogr. Y Cienc. Soc.* **2015**, *19*. [[CrossRef](#)]
27. Fletcher, C.H.; Romine, B.M.; Genz, A.S.; Barbee, M.M.; Dyer, M.; Anderson, T.R.; Lim, S.C.; Vitousek, S.; Bochicchio, C.; Richmond, B.M. *National Assessment of Shoreline Change: Historical Shoreline Change in the Hawaiian Islands*; USGS Publications Warehouse: Reston, VA, USA, 2012.
28. Salman, A.; Lombardo, S.; Doody, P. *Living with Coastal Erosion in Europe: Sediment and Space for Sustainability*; Technical Report; EUCC: Warnemünde, Germany, 2004.
29. Ponte Lira, C.; Nobre Silva, A.; Taborda, R.; Freire de Andrade, C. Coastline evolution of Portuguese low-lying sandy coast in the last 50 years: An integrated approach. *Earth Syst. Sci. Data* **2016**, *8*, 265–278. [[CrossRef](#)]
30. Guisado, E.; Malvárez, G.C.; Navas, F. Morphodynamic environments of the Costa del Sol, Spain. *J. Coast. Res.* **2013**, *65*, 500–506. [[CrossRef](#)]
31. Manno, G.; Anfuso, G.; Messina, E.; Williams, A.T.; Suffo, M.; Liguori, V. Decadal evolution of coastline armouring along the Mediterranean Andalusia littoral (South of Spain). *Ocean Coast. Manag.* **2016**, *124*, 84–99. [[CrossRef](#)]
32. Zviely, D.; Klein, M. The environmental impact of the Gaza Strip coastal constructions. *J. Coast. Res.* **2003**, *19*, 1122–1127.
33. Anfuso, G.; Dominguez, L.; Gracia, F. Short and medium-term evolution of a coastal sector in Cadiz, SW Spain. *Catena* **2007**, *70*, 229–242. [[CrossRef](#)]
34. Anfuso, G.; Martínez-del Pozo, J.; Rangel-Buitrago, N. Bad practice in erosion management: The southern Sicily case study. In *Pitfalls of Shoreline Stabilization: Selected Case Studies*; Cooper, J.A.G., Pilkey, O.H., Eds.; Springer: Dordrecht, The Netherlands, 2012; pp. 215–233.
35. Antony, E.; Sabatier, F. *Coastal Stabilization Practice in France*; Earthscan Routledge: London, UK, 2013; p. 253.
36. Anthony, E.J. The Human influence on the Mediterranean coast over the last 200 years: A brief appraisal from a geomorphological perspective. *Géomorphol. Relief Process. Environ.* **2014**, *20*, 219–226. [[CrossRef](#)]
37. Berlanga-Robles, C.A.; Ruiz-Luna, A. Land use mapping and change detection in the coastal zone of northwest Mexico using remote sensing techniques. *J. Coast. Res.* **2002**, *18*, 514–522.
38. Sabatier, F.; Samat, O.; Brunel, C.; Heurtefeux, H.; Delanghe-Sabatier, D. Determination of set-back lines on eroding coasts. Example of the beaches of the Gulf of Lions (French Mediterranean Coast). *J. Coast. Conserv.* **2009**, *13*, 57. [[CrossRef](#)]
39. Prieto, A.; Ojeda, J.; Rodríguez, S.; Gracia, J.; Del Río, L. Procesos erosivos (tasas de erosión) en los deltas mediterráneos andaluces: Herramientas de análisis espacial (DSAS) y evolución temporal (servicios OGC). In *Tecnologías de la Información Geográfica en el Contexto del Cambio Global, Proceedings of the XV Congreso Nacional de Tecnologías de la Información Geográfica, Madrid, Spain, 19–21 September 2012*; Martínez Vega, J., Martín Isabel, P., Eds.; CSIC—Instituto de Economía, Geografía y Demografía: Madrid, Spain, 2012; pp. 185–193.
40. Félix, A.; Baquerizo, A.; Santiago, J.; Losada, M. Coastal zone management with stochastic multi-criteria analysis. *J. Environ. Manag.* **2012**, *112*, 252–266. [[CrossRef](#)]
41. Guisado, E.; Malvárez, G. Multiple scale morphodynamic mapping: Methodological considerations and applications for the coastal atlas of Andalusia. *J. Coast. Res.* **2009**, *56*, 1513–1517.
42. Molina, R.; Manno, G.; Lo Re, C.; Anfuso, G.; Ciraolo, G. Storm Energy Flux Characterization along the Mediterranean Coast of Andalusia (Spain). *Water* **2019**, *11*, 509. [[CrossRef](#)]
43. López, M.F.P. El clima de Andalucía. In *Geografía de Andalucía*; Ariel Geografía: Barcelona, Spain, 2003; pp. 137–173.
44. REDIAM Red, d.I.A.d.A. WMS, Tasas de erosión en el litoral andaluz. Available online: <http://www.juntadeandalucia.es> (accessed on 10 June 2019).
45. Thieler, E.R.; Himmelstoss, E.A.; Zichichi, J.L.; Ergul, A. *The Digital Shoreline Analysis System (DSAS) Version 4.0—An ArcGIS Extension for Calculating Shoreline Change*; Technical Report; US Geological Survey: Reston, VA, USA, 2009.
46. Anfuso, G.; Bowman, D.; Danese, C.; Pranzini, E. Transect based analysis versus area based analysis to quantify shoreline displacement: Spatial resolution issues. *Environ. Monit. Assess.* **2016**, *188*, 568. [[CrossRef](#)] [[PubMed](#)]

47. Thieler, E.; Himmelstoss, E.; Zichichi, J.; Ergul, A. *DSAS 4.0 Installation Instructions and User Guide*, 4th ed.; U.S. Geological Survey Open-File Report 2008-1278; U.S. Geological Survey: Reston, VA, USA, 2009.
48. Dolan, R.; Fenster, M.S.; Holme, S.J. Temporal analysis of shoreline recession and accretion. *J. Coast. Res.* **1991**, *7*, 723–744.
49. Manno, G.; Re, C.L.; Ciraolo, G. Uncertainties in shoreline position analysis: The role of run-up and tide in a gentle slope beach. *Ocean Sci.* **2017**, *13*, 661. [[CrossRef](#)]
50. Moore, L.J. Shoreline mapping techniques. *J. Coast. Res.* **2000**, *16*, 111–124.
51. Dolan, R.; Hayden, B.P.; May, P.; May, S. The reliability of shoreline change measurements from aerial photographs. *Shore Beach* **1980**, *48*, 22–29.
52. Douglas, B.C.; Crowell, M. Long-term shoreline position prediction and error propagation. *J. Coast. Res.* **2000**, *16*, 145–152.
53. Pajak, M.J.; Leatherman, S. The high water line as shoreline indicator. *J. Coast. Res.* **2002**, *18*, 329–337.
54. Boak, E.H.; Turner, I.L. Shoreline definition and detection: A review. *J. Coast. Res.* **2005**, *21*, 688–703. [[CrossRef](#)]
55. Fisher, J.S.; Overton, M.F. Interpretation of shoreline position from aerial photographs. *Coast. Eng. Proc.* **1994**, *1*. [[CrossRef](#)]
56. Del Río, L.; Gracia, F.J. Error determination in the photogrammetric assessment of shoreline changes. *Nat. Hazards* **2013**, *65*, 2385–2397. [[CrossRef](#)]
57. Jabaloy, A.; Lobo, F.J.; Bárcenas, P.; Azor, A.; Fernández-Salas, L.M.; Díaz del Río, V. Evolución reciente del delta del Río Adra (SE España). *Geo-Temas* **2008**, *10*, 743–746.
58. Martínez, A.B. Tratamiento técnico del borde litoral almeriense. In *Actas de las Jornadas sobre el Litoral de Almería: Caracterización, Ordenación y Gestión de un Espacio Geográfico Celebradas en Almería, 20 a 24 de Mayo de 1997*; Instituto de Estudios Almerienses: Almería, Spain, 1999; pp. 207–232.
59. Viciano, A.M.L. La costa de Almería: Desarrollo socio-económico y degradación físico-ambiental (1957–2007). *Paralelo 37º* **2007**, *19*, 149–183.
60. Syvitski, J.P.; Vörösmarty, C.J.; Kettner, A.J.; Green, P. Impact of humans on the flux of terrestrial sediment to the global coastal ocean. *Science* **2005**, *308*, 376–380. [[CrossRef](#)]
61. Kim, J.; Choi, J.; Choi, C.; Hwang, C. Forecasting the potential effects of climatic and land-use changes on shoreline variation in relation to watershed sediment supply and transport. *J. Coast. Res.* **2016**, *33*, 874–888. [[CrossRef](#)]
62. Frihy, O.E. Nile Delta shoreline changes: Aerial photographic study of a 28-year period. *J. Coast. Res.* **1988**, *4*, 597–606.
63. Frihy, O.E.; Komar, P.D. Patterns of beach-sand sorting and shoreline erosion on the Nile Delta. *J. Sediment. Res.* **1991**, *61*, 544–550.
64. Pranzini, E. Airborne LIDAR survey applied to the analysis of the historical evolution of the Arno River delta (Italy). *J. Coast. Res.* **2007**, *50*, 400–409.
65. González, J.M.S.; Malvárez, G. La desembocadura del río Vélez (provincia de Málaga, España). Evolución reciente de un delta de comportamiento mediterráneo. *Rev. C G* **2003**, *17*, 47–61.
66. Malvarez, G.; Pollard, J.; Rodriguez, R.D. Origins, management, and measurement of stress on the coast of southern Spain. *Coast. Manag.* **2000**, *28*, 215–234.
67. Guisado-Pintado, E.; Malvárez, G. El rol de las tormentas en la evolución morfodinámica del Delta del río Vélez: Costa del Sol, Málaga. In *Geo-Temas*; Sociedad Geológica de España: Marbella, Spain, 2015; Volume 15, pp. 189–192.
68. Del Río, J.; Malvárez, G.; Navas, F. Aportes sedimentarios fluviales en el sistema litoral y su importancia para la gestión de costas: El caso de la Ensenada de Marbella. In *Análisis Espacial Y Representación Geográfica: Innovación Y Aplicación*; Universidad Pablo de Olavide: Sevilla, Spain, 2015; pp. 2175–2177.
69. Del Río, J.L.; Malvárez, G. Impacto de la regulación del río Verde en la erosión del sistema sedimentario litoral de la ensenada de Marbella, Costa del Sol. In *XV Coloquio Ibérico de Geografía*; Universidad de Murcia: Murcia, Spain, 2016; pp. 1–10.
70. Del Río, J.; García, G.M. Erosión costera y acumulación de sedimentos en los embalses: El caso de La Concepción en la Ensenada de Marbella, Málaga. *Geotemas* **2017**, *17*, 251–254.
71. Valdemoro, H.I.; Jiménez, J.A. The influence of shoreline dynamics on the use and exploitation of Mediterranean tourist beaches. *Coast. Manag.* **2006**, *34*, 405–423. [[CrossRef](#)]

72. Dehouck, A.; Dupuis, H.; Sénéchal, N. Pocket beach hydrodynamics: The example of four macrotidal beaches, Brittany, France. *Mar. Geol.* **2009**, *266*, 1–17. [[CrossRef](#)]
73. Bray, M.J.; Carter, D.J.; Hooke, J.M. Littoral cell definition and budgets for central southern England. *J. Coast. Res.* **1995**, *11*, 381–400.
74. Pranzini, E.; Anfuso, G.; Cinelli, I.; Piccardi, M.; Vitale, G. Shore Protection Structures Increase and Evolution on the Northern Tuscany Coast (Italy): Influence of Tourism Industry. *Water* **2018**, *10*, 1647. [[CrossRef](#)]
75. Sanuy, M.; Jiménez, J.A. Sensitivity of Storm-Induced Hazards in a Highly Curvilinear Coastline to Changing Storm Directions. The Tordera Delta Case (NW Mediterranean). *Water* **2019**, *11*, 747. [[CrossRef](#)]
76. Griggs, G.B. The impacts of coastal armoring. *Shore Beach* **2005**, *73*, 13–22.
77. Dugan, J.; Airolidi, L.; Chapman, M.; Walker, S.; Schlacher, T.; Wolanski, E.; McLusky, D. 8.02-Estuarine and coastal structures: Environmental effects, a focus on shore and nearshore structures. In *Treatise on Estuarine and Coastal Science*; Wolanski, E., McLusky, D.S., Eds.; Academic Press: Waltham, MA, USA, 2011; Volume 8, pp. 17–41.
78. Nordstrom, K.F. *Beaches and Dunes of Developed Coasts*; Cambridge University Press: Cambridge, UK, 2000.
79. Miles, J.R.; Russell, P.E.; Huntley, D.A. Field measurements of sediment dynamics in front of a seawall. *J. Coast. Res.* **2001**, *17*, 195–206.
80. Anfuso, G.; Martínez-del Pozo, J.Á.; Rangel-Buitrago, N. Morphological cells in the Ragusa littoral (Sicily, Italy). *J. Coast. Conserv.* **2013**, *17*, 369–377. [[CrossRef](#)]
81. Cooper, J.; Anfuso, G.; Del Río, L. Bad beach management: European perspectives. *Geol. Soc. Am. Ser.* **2009**, *460*, 167–179.
82. Wiggins, M.; Scott, T.; Masselink, G.; Russell, P.; Valiente, N.G. Regionally-Coherent Embayment Rotation: Behavioural Response to Bi-Directional Waves and Atmospheric Forcing. *J. Mar. Sci. Eng.* **2019**, *7*, 116. [[CrossRef](#)]
83. Burningham, H.; French, J. Understanding coastal change using shoreline trend analysis supported by cluster-based segmentation. *Geomorphology* **2017**, *282*, 131–149. [[CrossRef](#)]



© 2019 by the authors. Licensee MDPI, Basel, Switzerland. This article is an open access article distributed under the terms and conditions of the Creative Commons Attribution (CC BY) license (<http://creativecommons.org/licenses/by/4.0/>).